Biochimica et Biophysica Acta 1838 (2014) 231–236

Contents lists available at ScienceDirect

Biochimica et Biophysica Acta

journal homepage: www.elsevier.com/locate/bbamem

The third intracellular loop plays a critical role in bitter taste receptor activation

Sai Prasad Pydi, Nisha Singh, Jasbir Upadhyaya, Rajinder Pal Bhullar, Prashen Chelikani *

Department of Oral Biology, University of Manitoba, The Manitoba Institute of Child Health, Winnipeg, MB R3E 0W4, Canada

ARTICLE INFO

Article history:
Received 18 March 2013
Received in revised form 12 August 2013
Accepted 14 August 2013
Available online 29 August 2013

Keywords:
G protein-coupled receptors (GPCRs)
Bitter taste receptors (T2Rs)
Intracellular loops (ICLs)
Constitutive activity
Molecular modeling

ABSTRACT

Bitter taste receptors (T2Rs) belong to the superfamily of G protein-coupled receptors (GPCRs). T2Rs are chemosensory receptors with important therapeutic potential. In humans, bitter taste is perceived by 25 T2Rs, which are distinct from the well-studied Class A GPCRs. The activation mechanism of T2Rs is poorly understood and none of the structure–function studies are focused on the role of the important third intracellular loop (ICL3). T2Rs have a unique signature sequence at the cytoplasmic end of fifth transmembrane helix (TM5), a highly conserved LxxSL motif. Here, we pursue an alanine scan mutagenesis of the ICL3 of T2R4 and characterize the functionality of 23 alanine mutants. We identify four mutants, H214A, Q216A, V234A and M237A, that exhibit constitutive activity. To our surprise, the H214A mutant showed very high constitutive activity over wild type T2R4. Interestingly, His214 is highly conserved (96%) in T2Rs and is present two amino acids below the LxxSL motif in TM5. Molecular modeling shows a dynamic network of interactions involving residues in TM5–ICL3–TM6 that restrain the movement of the helices. Changes in this network, as in the case of H214A, Q216A, V234A and M237A mutants, cause the receptor to adopt an active conformation. The conserved LxxSL motif in TM5 performs both structural and functional roles in this process. These results provide insight into the activation mechanism of T2Rs, and emphasize the unique functional role of ICL3 even within the GPCR subfamilies.

1. Introduction

Humans can sense five basic tastes. Among these, sweet, umami and bitter tastes are sensed by chemosensory receptors that belong to the G protein-coupled receptor (GPCR) superfamily [1,2]. Sweet taste signals are transduced by a heterodimer of T1R2 and T1R3, while the T1R1 and T1R3 heterodimer codes for the umami taste [1,3,4]. The three receptor subunits (T1Rs), T1R1, T1R2 and T1R3, that code for sweet and umami tastes belong to the class C GPCR family [2]. Class C GPCRs, which include the metabotropic receptors, are characterized by a large N-terminal domain, also known as the venus flytrap (VFT), that forms the primary (orthosteric) ligand binding site [2]. In contrast, the 25 bitter taste receptors (T2Rs) in humans have a short N-terminus [5,6] and the ligand binds within the transmembrane (TM) domain [7,8]. The classification of T2Rs within the GPCR superfamily is unclear with some grouping them with frizzled receptors (FZD) [2], whereas others place them separately [9]. However, the International Union of Basic and Clinical Pharmacology (IUPHAR) list FZD as a separate GPCR family, Class F or Frizzled, and this class does not include T2Rs [10]. Amino acid sequence analysis of T2Rs showed that the conserved motifs such as the D/ERY in TM3 and CWxP in TM6 are absent in T2Rs [11]. Mutational studies of the highly conserved residues in the TM domain of T2Rs suggest that these receptors might have a unique activation mechanism compared to other classes of the GPCR superfamily [11,12].

Recently, we identified a conserved LxxSL motif in TM5 of T2Rs. Mutational and molecular modeling analysis of this motif suggested that it performs a structural role by stabilizing the helical conformation of TM5 at the cytoplasmic end [11]. However, the LxxSL motif is present very close to the third intracellular loop (ICL3) and role of this loop in T2R activation has not been studied thus far. ICL3 was found to perform different roles in different GPCR classes. For example in Ste2p, a yeast GPCR, disulfide cross-linking experiments show that the cytoplasmic ends of TM5 and TM6 that flank ICL3 undergo conformational changes upon ligand binding, whereas the center of the ICL3 loop does not [13]. In neuropeptide Y1 receptor (NPY1), ICL3 constrains the inactive state of the receptor, and mutations in ICL3 lead to an agonist-independent or basal or constitutive activity [14]. In contrast, a recent alanine scan mutagenesis of ICL3 in the melanocortin-3 receptor (MC3R) showed that ICL3 is important for ligand binding and signaling, but none of the mutants displayed constitutive activity [15].

In this report, we have examined the molecular determinants in ICL3 which are required for bitter taste receptor activation and signaling. In addition, we studied the interactions between the conserved LxxSL motif and ICL3 in T2Rs. To elucidate this, we performed alanine scan mutagenesis of ICL3 and functionally characterized 23 alanine mutants of T2R4. Our results, which are based on site-directed mutagenesis, pharmacological characterization of the mutants and molecular modeling

* Corresponding author at: D319, Department of Oral Biology, 780 Bannatyne Avenue, University of Manitoba, Winnipeg, MB R3E 0W4, Canada. Tel.: +1 204 789 3539; fax: +1 204 789 3913.
E-mail address: Prashen.Chelikani@ad.umanitoba.ca (P. Chelikani).

0005-2736/$ – see front matter © 2013 Elsevier B.V. All rights reserved.
http://dx.doi.org/10.1016/j.bbamem.2013.08.009

analysis, allowed us to identify four constitutively active mutants (CAMs) in ICL3, with constitutive activity ranging from 2 to 10 fold over wild type T2R4. Taken together, our results showed that the cytoplasmic ends of TM5 and TM6 played an important role in T2R activation, and ICL3 was involved in restraining T2Rs in an inactive conformation.

2. Materials and methods

2.1. Materials

Calcium sensitive dye Fluo-4NW and cell culture media were purchased from Invitrogen (Carlsbad, CA, USA). IP3 kit was from DiscoveRx (Fremont, CA, USA). Fetal bovine serum (FBS), quinine, denatonium benzoate, colchicine, yohimbine and common chemicals were purchased from Sigma. The Gα16-gust44 chimera was a gift from Dr. Takashi Ueda, Nagoya City University, Japan.

2.2. Molecular biology

The synthetic and N-terminal FLAG tagged TAS2R4 gene in the mammalian expression vector pcDNA3.1 (Invitrogen) was described before [12]. Alanine mutants were introduced into this gene using a commercial service (GenScript Inc., USA). The wild type and mutant TAS2R4 genes in pcDNA3.1 were transiently co-transfected along with Gα16-gust44 chimera in HEK293T cells using lipofectamine 2000 (Invitrogen) as described previously [12].

2.3. Functional assays

Cell surface ELISA, calcium mobilization assays, IP3 assays, and pharmacological characterization of CAMs were performed according to previously published protocols [11,12,16].

2.4. Molecular modeling

The inactive and CAM models of T2R4 were built by homology modeling as described before [12]. The models were minimized using the steepest descent and conjugate gradient algorithms. MD simulations of 10 ns were carried out with time-step of 2 fs, collecting trajectory data every 500 ps. Simulations were carried out using SYBYL X v2.1 modeling suite (Tripos Inc., USA).

3. Results

Structure–function analysis of T2Rs revealed unique signature residues in TM helices which are distinct from Class A GPCRs [11,12]. Our previous structure–function studies on T2R4 targeted the N-terminus and TM regions that play a role in receptor expression and activation [12,17]. The intracellular region of T2R4 consists of 87 amino acids which includes four alanines. In this report, using an N-terminal FLAG tagged T2R4 (WT-T2R4) as the base receptor, the entire T2R4–ICL3 region consisting of 23 amino acids was replaced with alanines and the mutants were characterized biochemically (Fig. 1).

3.1. Functional characterization

The natural alkaloid, quinine, acts as an agonist and activates T2R4 in a concentration dependent manner [12,18]. It is one of the well-characterized agonists of T2R4 and has been used in this study. Taste sensory analysis of a few bitter compounds has reported quinine as the most intense bitter compound [11]. The 23 alanine mutants in ICL3 of T2R4 displayed varied levels of calcium mobilization upon stimulation with quinine (Table 1). Only 14 of the 23 ICL3 alanine mutants displayed quinine induced signaling in a concentration dependent manner (Table 1). Three ICL3 mutants, Q216A, T230A and V234A, showed an increase in agonist induced response; however, their response was not

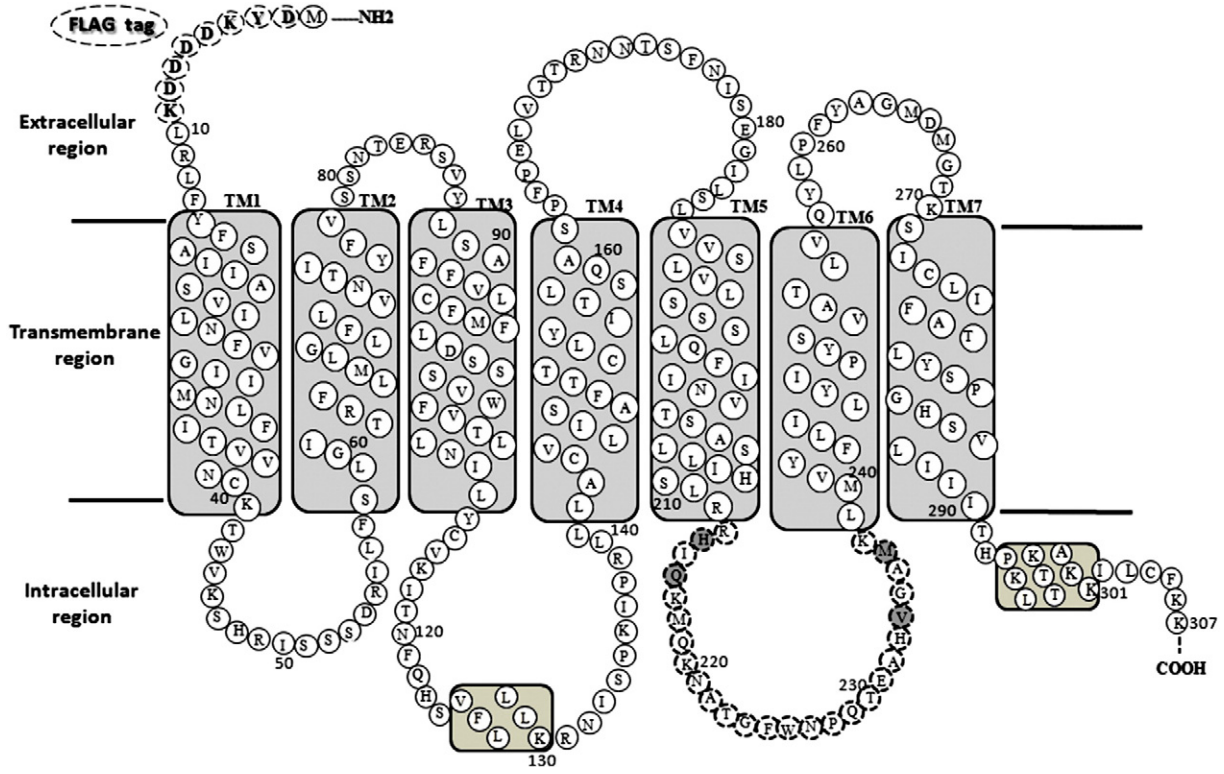

Fig. 1. Two-dimensional representation of the T2R4 amino acid sequence with FLAG-tag at the N-terminus. The receptor consists of seven transmembrane (TM) helices, a short N-terminus, three extracellular loops (ECLs) and three intracellular loops (ICLs), and a cytoplasmic tail. The 23 ICL3 residues mutated to alanine in this study are displayed in broken rings. The constitutively active mutants identified in this study are represented in gray circles.

Table 1
Pharmacological characterization of the T2R4 alanine mutants. Functional characterization of the mutants was pursued by measuring intracellular calcium mobilized after stimulating with different concentrations of agonist, quinine. Cell surface expression was determined by ELISA.[a]

Mutant	EC_{50} (μM)	EC_{50} mutant/EC_{50} wild type	Cell surface expression (%)
T2R4	997 ± 416	1.0	100 ± 3
R213A	ND		133 ± 2
H214A	1345 ± 553	1.30	102 ± 8
I215A	2043 ± 1215	2.05	78 ± 1
Q216A	NS		133 ± 20
K217A	1599 ± 1148	1.59	101 ± 21
M218A	1133 ± 512	1.13	121 ± 4
Q219A	ND		109 ± 12
K220A	ND		112 ± 29
N221A	1432 ± 674	1.43	118 ± 38
T223A	1339	1.34	106 ± 2
G224A	1638 ± 820	1.62	111 ± 36
F225A	1946 ± 656	1.95	105 ± 3
W226A	1213 ± 249	1.21	115 ± 10
N227A	1509 ± 977	1.51	99 ± 15
P228A	2756 ± 1308	2.75	100 ± 25
Q229A	ND		101 ± 13
T230A	NS		107 ± 47
E231A	ND		110 ± 6
H233A	ND		145 ± 12
V234A	NS		107 ± 15
G235A	890 ± 452	0.89	139 ± 20
M237A	832 ± 567	0.83	106 ± 14
K238A	1822 ± 1170	1.82	143 ± 24

[a] Intracellular loop 3 (ICL3). ND — not detected, no significant calcium mobilization detected; NS — not saturated, quinine concentration dependent increase in calcium mobilization not observed.

saturated even at the highest concentration of 5 mM quinine (Table 1). Concentrations higher than 5 mM resulted in significant increase in non-specific calcium mobilization in cells, expressing the WT-T2R4 or mutants (data not shown). The R213A, Q219A, K220A, Q229A, E231A and H233A mutants, upon stimulation with quinine, showed no detectable or statistically significant increase in intracellular calcium mobilization when compared to mock transfected cells. Fig. 2 shows representative calcium traces for select mutants and mock transfected cells stimulated with a saturating concentration of 2.5 mM quinine. Interestingly, I215A, F225A and P228A displayed altered receptor activation and/or defective ligand binding, as shown by a 2-fold increase in EC_{50} mutant/wild type ratio (Table 1). For these three mutants, signal was saturated at only the highest quinine concentration of 5 mM (one saturating data point), and their EC_{50} values were calculated by non-linear regression analysis using PRISM software version 4.03 (GraphPad Software Inc., San Diego, CA). The threshold values (defined as the lowest quinine concentration at which a specific calcium signal was observed) for these mutants were 550 μM, 645 μM and 850 μM respectively, compared to 200 μM for WT-T2R4. Cell surface ELISA revealed that all the ICL3 mutants were expressed on the surface with expression levels ranging from 80% to 140% of WT-T2R4.

3.2. Identification and characterization of CAMs in T2R4-ICL3

To obtain insights into the role of intracellular residues in T2R activation, we characterized the agonist-independent (basal) activity of WT-T2R4 and all the 23 alanine mutants. Basal Ca^{2+} levels of WT-T2R4 and the mutants corrected for cell surface expression were measured to assess the agonist-independent activity (Fig. 3). Mutants R213A, H214A, Q216A, N227A, V234A and M237A showed statistically significant increased basal signaling (Fig. 3A). Since H214A shows the highest basal activity in terms of calcium mobilized among the 23 alanine replacements, this mutant was selected for further study. To obtain direct evidence of the constitutive activity of H214A, we measured the basal IP3 of WT-T2R4 and H214A mutant (Fig. 3B). A standard graph was constructed using different concentrations of IP3 provided by the manufacturer, and this graph was used to calculate the amount of IP3 released by the wild type and mutant receptor, and as described before [16]. IP3 levels of both receptors were measured by stimulating them with buffer (agonist independent or basal) and these values were normalized to cell surface expression of WT-T2R4 and H214A. When compared to WT-T2R4, a 3-fold increase was observed in agonist independent activity of H214A, and the significant p value was less than 0.01 (Fig. 3B).

The effect of receptor density on Ca^{2+} mobilization was calculated from slope of expression vs. basal activity for the six mutants that showed high basal signaling and compared to WT-T2R4. The results based on the slope values showed that only H214A, Q216A, V234A and M237A mutants exhibited a true CAM phenotype, with constitutive activity ranging from 2 to 10 fold over WT-T2R4 (Fig. 3C). The H214A mutant present at the TM5–ICL3 interface displayed the highest constitutive activity. Interestingly, His214 is present in 24 of the 25 human T2Rs (96% sequence conserved).

3.3. Analysis of molecular models

To interpret the effect of ICL3 CAMs on T2R4 structure and function, we built homology models of the inactive WT-T2R4, a constitutively active T2R4 and CAMs using rhodopsin inactive (PDB ID: 1U19) and CAM (PDB ID: 2X72) crystal structures as templates. The four CAMs in ICL3 identified in this study are present at the amino and carboxyl-terminus of T2R4-ICL3. Through an intricate network that involves side-chain and backbone interactions, His214, Gln216, Val234 and Met237 interact with the highly conserved LxxSL motif on TM5 (Fig. 4

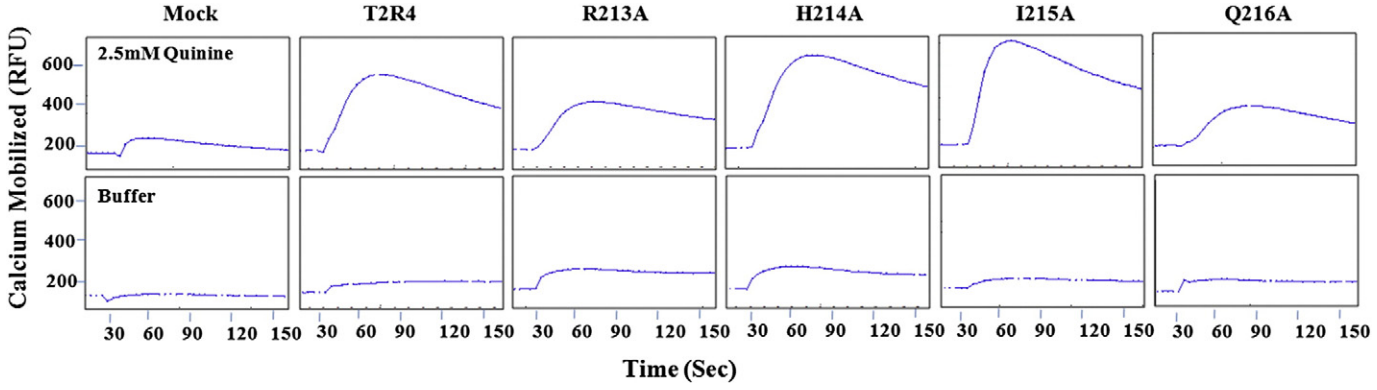

Fig. 2. Representative calcium traces for HEK293T cells transiently transfected with T2R4 and select mutants. The mock transfected (pcDNA) control is shown. The cells were stimulated with 2.5 mM quinine (top panel) or assay buffer (lower panel). The calcium mobilized (RFUs or Relative Fluorescence Units) was detected using the calcium sensitive dye Fluo 4NW (Invitrogen), and fluorescence measured using Flex Station III microplate reader as described before [12].

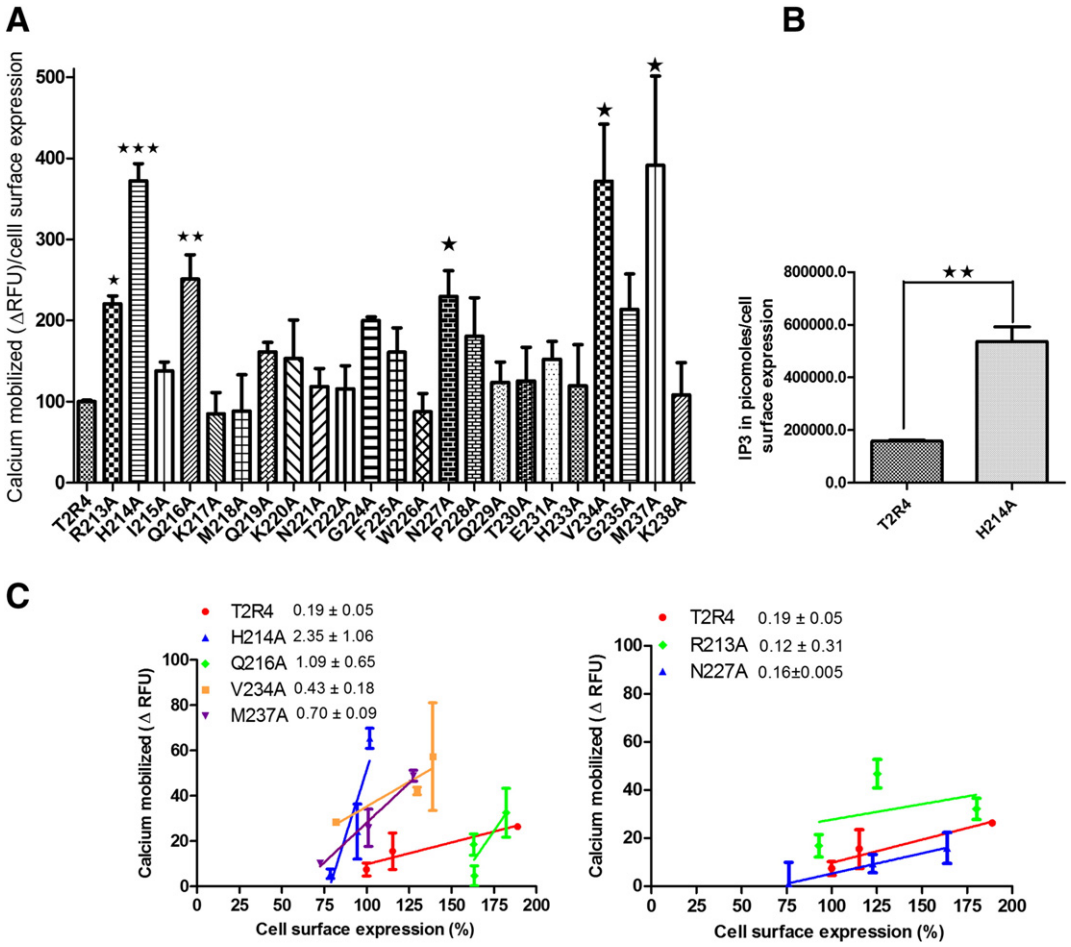

Fig. 3. A. Pharmacological characterization of the basal or agonist independent activity of WT-T2R4 and intracellular alanine mutants. Calcium mobilized (ΔRFU) was normalized to WT-T2R4 cell surface expression as determined by ELISA. The results were analyzed using one way ANOVA with *Tukey's* post hoc test, at significance level $p < 0.05$. B. Basal or agonist independent IP3 accumulation is represented (bar plots) by normalizing to cell surface expression determined by ELISA. Results are from three independent experiments performed in triplicate. The results were analyzed using Student *t*-test at a significance level $p < 0.05$. C. Effect of receptor density on basal calcium mobilization. The H214A, Q216A, V234A and M237A mutants displayed true constitutive activity. The slope values of the constitutively active mutants (CAMs) are shown next to the mutant. The H214A (2.35 ± 1.06) displayed the highest constitutive activity, with greater than 10-fold increase in basal activity over WT-T2R4 (0.19 ± 0.05).

and Supplementary Fig. 1). Analysis of the molecular models suggests a major rearrangement at the cytoplasmic ends of TM5 and TM6 (see Discussion).

4. Discussion

In GPCRs, important structural and sequence differences within receptors from different classes suggest distinct activation mechanisms. One of the earliest reported biophysical studies directed at understanding the conformational changes in GPCRs was that of rhodopsin. Site-directed spin label studies on rhodopsin suggested the 'helix movement model' of GPCR activation, which showed that, upon receptor activation, TM6 moved away from the 7-TM bundle [19]. This study was corroborated more than a decade later by crystal structures of the inactive and active states of various Class A GPCRs. In class A GPCRs, comparison of the recent crystal structures of agonist-bound active states of rhodopsin [20], the β2 adrenergic receptor (β_2AR) [21], and the A_{2A} adenosine receptor (A_{2A}AR) [22], shows that activation of these GPCRs results in rearrangements of TM5 and TM6. However, the extent of this conformational change varies. For example, depending on whether stabilizers of the active conformation were used, such as C-terminal peptide of the transducin in case of rhodopsin, or conformationally selective nanobody in case of β_2AR or none in case of A_{2A}AR, movement of the cytoplasmic side of TM6 ranges between 3 Å in A_{2A}AR to 8 Å in β_2AR [23]. The Arg of the D/ERY motif in TM3 of most Class A GPCRs makes an ionic interaction with a conserved acidic residue (D/E) of TM6. This lock stabilizes the inactive state of many class A GPCRs. However, D/ERY motif is not found in GPCRs from other classes.

The Class C and Class F GPCRs show divergence from Class A in both amino acid sequence and pharmacological properties [10,24]. The Class C GPCRs predominantly include the metabotropic glutamate receptors (mGluRs), γ-aminobutyric acid (GABA) receptors and the T1Rs. A representative structure of a Class C GPCR is still not available. Recently the structure of a non-Class A GPCR, the smoothened (SMO) receptor, which belongs to Class F was elucidated [25]. This structure of the SMO receptor bound to a small antagonist molecule reveals an unusually complex arrangement of long extracellular loops stabilized by four disulphide bonds. Despite the overall structural conservation of the 7-TM fold with the Class A GPCRs, the structure of the SMO receptor reveals many unique features. Most importantly TM5, TM6 and TM7, of the SMO receptor lack the highly conserved prolines ($P^{5.50}$, $P^{6.50}$ and $P^{7.50}$) [26], which play pivotal roles in Class A GPCR activation. It seems, even in the absence of the conserved Class A GPCRs motifs, including D/ERY in TM3, CWxP in TM6 and NPxxY in TM7 in Class F GPCRs, there are some common structural features among the different GPCR classes which stabilize the inactive state.

Recent molecular modeling studies using BiHelix and SuperBiHelix Monte Carlo methods on T2R38 predicted the hydrogen bond interactions between TM3 and TM6 or between TM5 and TM6 to play a role in receptor activation [27]. Results from our studies suggest that the

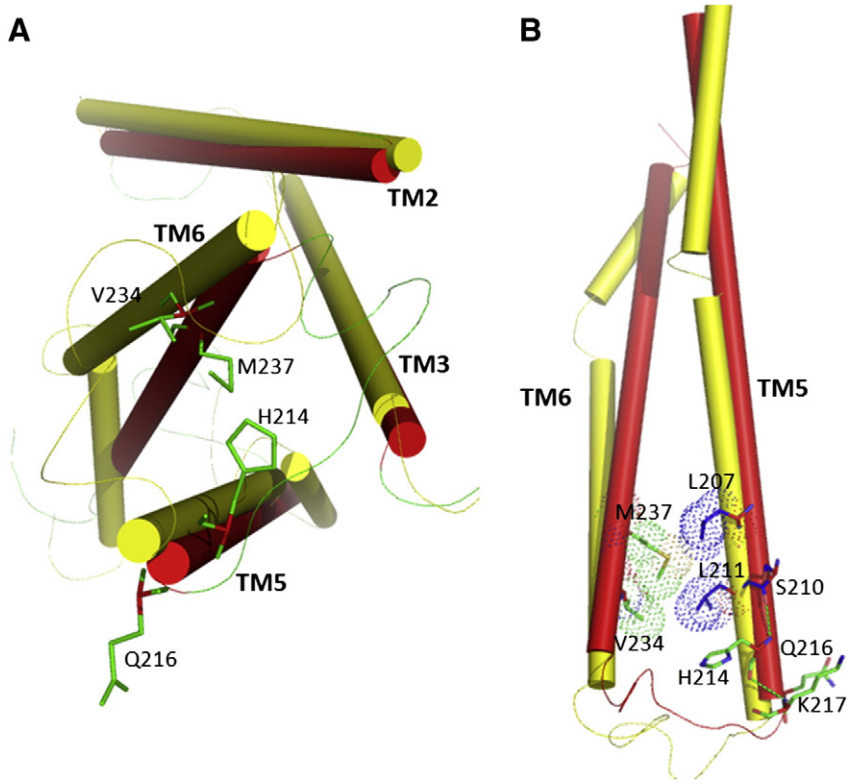

Fig. 4. Homology models of the inactive (red) and constitutively active (yellow) T2R4 were built using the rhodopsin inactive (PDB ID: 1U19) and CAM (PDB ID: 2X72) structures as templates. A. The left panel shows the intracellular view (from the cytoplasmic side) of TM2–TM3–TM5–TM6 arrangement in both the T2R4 structures. The intracellular loops (ICLs), along with the location of the ICL3 CAMs, are shown as threads. B. The right panel shows the membrane view of TM5–TM6, along with ICL3 CAMs and the packing interactions of the LxxSL motif on TM5. In the T2R4 CAM model, the cytoplasmic end of TM6 moves by around 2 Å towards the helical core.

cytoplasmic end of TM6 moves 2 Å, while no major changes were observed in the movement of TM5. Previously, we have reported that the highly conserved LxxSL motif in T2R1 has an important structural role in stabilizing the helical conformation of TM5 [11]. Results from this study suggest that residues of the LxxSL motif also perform a functional role by forming a network of hydrogen-bond interactions with residues present in ICL3 and TM6, including the highly conserved His214 (96% conserved in T2Rs). Therefore, the conserved LxxSL motif at the cytoplasmic end of TM5 plays both a structural and functional role in T2Rs. In the inactive T2R4 model, Leu207 and Ser210 of the LxxSL interact with Met237 and His214 respectively. In the CAM model, His214 interacts with the side chain of Ser210 and backbone of Leu211, while the side chain of Met237 moves away from Lue207 to interact with Leu211 (Supplementary Fig. 1). Unfortunately, our molecular models gave limited insights into the interactions of the ICL3 residues; this can be due to a number of factors. For example, it is well known that loops are the most flexible regions in GPCRs and predicting the conformation of the loop is very difficult. In addition, the binding of intracellular proteins including G-protein(s), on the intracellular side of T2Rs, might cause conformational changes in the ICLs, which cannot be predicted by the molecular models.

There is a dearth of ligands with good efficacy for T2R4. Previously, T2R4 was shown to be activated by 15 bitter compounds, with only the arbitrary threshold values for activation reported, except for colchicine [28]. We tested the pharmacology profile of four of those ligands; quinine, denatonium benzoate, colchicine and yohimbine and found only two of them activating T2R4 (data not shown). Denatonium benzoate and quinine activate T2R4 with EC_{50} values of 23 mM and 1 mM respectively [18]. Whereas, colchicine and yohimbine were unable to show any significant activation of the receptor in our assay conditions. In this study, there were a number of mutants, which showed no detectable signal, or the signal was not saturated even with 5 mM quinine and few mutants showed high EC_{50} values. We speculate that the conformational changes in the receptor brought about by these mutations might have altered the ligand binding pocket, thereby affecting quinine binding. It is possible that the signal might be rescued when induced with a different ligand. However, in the absence of other well-characterized agonists and antagonists of T2R4, this aspect could not be pursued further. Similarly, for the mutants that showed high EC_{50} mutant/wild type ratio, whether this loss in function resulted because of altered receptor activation and/or defective ligand binding, could not be characterized for now.

5. Conclusions

Our results show that the network of interactions involving conserved residues at the cytoplasmic ends of TM5 and TM6 play an important role in stabilizing the inactive state of T2Rs. Changes in this network, brought about by mutations such as H214A, lead the receptor to adopt an active conformation which involves the movement of TM6. The H214A mutant shows constitutive activity of up to 10-fold over WT-T2R4 based on slope values determined by calculating the effect of receptor density on calcium mobilization, one of the highest reported for a GPCR mutant. This study opens up new areas of research on bitter taste signaling. Development of assays for the CAMs identified in this study would allow pharmacological characterization of novel bitter taste blockers into antagonists and inverse agonists.

Acknowledgments

This work was supported by a Discovery grant (RGPIN 356285) from the Natural Sciences and Engineering Research Council of Canada (NSERC), and a New Investigator Award from Heart and Stroke Foundation of Canada (HSFC) to PC. A University of Manitoba Graduate Fellowship to SP. SP, RB and PC has a patent application pending on bitter taste receptors.

Appendix A. Supplementary data

Supplementary data to this article can be found online at http://dx.doi.org/10.1016/j.bbamem.2013.08.009.

References

[1] M.A. Hoon, E. Adler, J. Lindemeier, J.F. Battey, N.J. Ryba, C.S. Zuker, Putative mammalian taste receptors: a class of taste-specific GPCRs with distinct topographic selectivity, Cell 96 (1999) 541–551.

[2] M.C. Lagerstrom, H.B. Schioth, Structural diversity of G protein-coupled receptors and significance for drug discovery, Nat. Rev. Drug Discov. 7 (2008) 339–357.

[3] G. Nelson, M.A. Hoon, J. Chandrashekar, Y. Zhang, N.J. Ryba, C.S. Zuker, Mammalian sweet taste receptors, Cell 106 (2001) 381–390.

[4] X. Li, L. Staszewski, H. Xu, K. Durick, M. Zoller, E. Adler, Human receptors for sweet and umami taste, Proc. Natl. Acad. Sci. U. S. A. 99 (2002) 4692–4696.

[5] J. Chandrashekar, K.L. Mueller, M.A. Hoon, E. Adler, L. Feng, W. Guo, C.S. Zuker, N.J. Ryba, T2Rs function as bitter taste receptors, Cell 100 (2000) 703–711.

[6] S. Prasad Pydi, J. Upadhyaya, N. Singh, R. Pal Bhullar, P. Chelikani, Recent advances in structure and function studies on human bitter taste receptors, Curr. Protein Pept. Sci. 13 (2012) 500–508.

[7] A. Brockhoff, M. Behrens, M.Y. Niv, W. Meyerhof, Structural requirements of bitter taste receptor activation, Proc. Natl. Acad. Sci. U. S. A. 107 (2010) 11110–11115.

[8] T. Sakurai, T. Misaka, M. Ishiguro, K. Masuda, T. Sugawara, K. Ito, T. Kobayashi, S. Matsuo, Y. Ishimaru, T. Asakura, K. Abe, Characterization of the beta-D-glucopyranoside binding site of the human bitter taste receptor hTAS2R16, J. Biol. Chem. 285 (2010) 28373–28378.

[9] B. Vroling, M. Sanders, C. Baakman, A. Borrmann, S. Verhoeven, J. Klomp, L. Oliveira, J. de Vlieg, G. Vriend, GPCRDB: information system for G protein-coupled receptors, Nucleic Acids Res. 39 (2010) D309–D319.

[10] J.L. Sharman, H.E. Benson, A.J. Pawson, V. Lukito, C.P. Mpamhanga, V. Bombail, A.P. Davenport, J.A. Peters, M. Spedding, A.J. Harmar, I. Nc, IUPHAR-DB: updated database content and new features, Nucleic Acids Res. 41 (2013) D1083–D1088.

[11] N. Singh, S.P. Pydi, J. Upadhyaya, P. Chelikani, Structural basis of activation of bitter taste receptor T2R1 and comparison with class a G-protein-coupled receptors (GPCRs), J. Biol. Chem. 286 (2011) 36032–36041.

[12] S.P. Pydi, R.P. Bhullar, P. Chelikani, Constitutively active mutant gives novel insights into the mechanism of bitter taste receptor activation, J. Neurochem. 122 (2012) 537–544.

[13] G.K. Umanah, L.Y. Huang, J.M. Maccarone, F. Naider, J.M. Becker, Changes in conformation at the cytoplasmic ends of the fifth and sixth transmembrane helices of a yeast G protein-coupled receptor in response to ligand binding, Biochemistry 50 (2011) 6841–6854.

[14] M.J. Chee, K. Morl, D. Lindner, N. Merten, G.W. Zamponi, P.E. Light, A.G. Beck-Sickinger, W.F. Colmers, The third intracellular loop stabilizes the inactive state of the neuropeptide Y1 receptor, J. Biol. Chem. 283 (2008) 33337–33346.

[15] Z.Q. Wang, Y.X. Tao, Functions of the third intracellular loop of the human melanocortin-3 receptor, Curr. Pharm. Des. 19 (2013) 4831–4838.

[16] R. Chakraborty, S.P. Pydi, S. Gleim, R.P. Bhullar, J. Hwa, S. Dakshinamurti, P. Chelikani, New insights into structural determinants for prostanoid thromboxane A2 receptor- and prostacyclin receptor-g protein coupling, Mol. Cell. Biol. 33 (2013) 184–193.

[17] S.P. Pydi, R. Chakraborty, R.P. Bhullar, P. Chelikani, Role of rhodopsin N-terminus in structure and function of rhodopsin-bitter taste receptor chimeras, Biochem. Biophys. Res. Commun. 430 (2013) 179–182.

[18] N. Singh, M. Vrontakis, F. Parkinson, P. Chelikani, Functional bitter taste receptors are expressed in brain cells, Biochem. Biophys. Res. Commun. 406 (2011) 146–151.

[19] D.L. Farrens, C. Altenbach, K. Yang, W.L. Hubbell, H.G. Khorana, Requirement of rigid-body motion of transmembrane helices for light activation of rhodopsin, Science 274 (1996) 768–770.

[20] J. Standfuss, P.C. Edwards, A. D'Antona, M. Fransen, G. Xie, D.D. Oprian, G.F. Schertler, The structural basis of agonist-induced activation in constitutively active rhodopsin, Nature 471 (2011) 656–660.

[21] D.M. Rosenbaum, C. Zhang, J.A. Lyons, R. Holl, D. Aragao, D.H. Arlow, S.G. Rasmussen, H.J. Choi, B.T. Devree, R.K. Sunahara, P.S. Chae, S.H. Gellman, R.O. Dror, D.E. Shaw, W.I. Weis, M. Caffrey, P. Gmeiner, B.K. Kobilka, Structure and function of an irreversible agonist-beta(2) adrenoceptor complex, Nature 469 (2011) 236–240.

[22] F. Xu, H. Wu, V. Katritch, G.W. Han, K.A. Jacobson, Z.G. Gao, V. Cherezov, R.C. Stevens, Structure of an agonist-bound human A2A adenosine receptor, Science 332 (2011) 322–327.

[23] X. Deupi, J. Standfuss, Structural insights into agonist-induced activation of G-protein-coupled receptors, Curr. Opin. Struct. Biol. 21 (2011) 541–551.

[24] N. Yanamala, K.C. Tirupula, J. Klein-Seetharaman, Preferential binding of allosteric modulators to active and inactive conformational states of metabotropic glutamate receptors, BMC Bioinforma. 9 (Suppl. 1) (2008) S16.

[25] C. Wang, H. Wu, V. Katritch, G.W. Han, X.P. Huang, W. Liu, F.Y. Siu, B.L. Roth, V. Cherezov, R.C. Stevens, Structure of the human smoothened receptor bound to an antitumour agent, Nature 497 (2013) 338–343.

[26] J.A. Ballesteros, H. Weinstein, Integrated methods for the construction of three dimensional models and computational probing of structure–function relations in G-protein coupled receptors, Methods Neurosci. 25 (1995) 366–428.

[27] J. Tan, R. Abrol, B. Trzaskowski, W.A. Goddard III, 3D structure prediction of TAS2R38 bitter receptors bound to agonists phenylthiocarbamide (PTC) and 6-n-propylthiouracil (PROP), J. Chem. Inf. Model. 52 (2012) 1875–1885.

[28] W. Meyerhof, C. Batram, C. Kuhn, A. Brockhoff, E. Chudoba, B. Bufe, G. Appendino, M. Behrens, The molecular receptive ranges of human TAS2R bitter taste receptors, Chem. Senses 35 (2010) 157–170.